ISSN 1068-798X, Russian Engineering Research, 2010, Vol. 30, No. 2, pp. 133–137. © Allerton Press, Inc., 2010.
Original Russian Text © S.I. Petrushin, A.V. Proskokov, 2010, published in Vestnik Mashinostroeniya, 2010, No. 2, pp. 40–44.

Theory of Constrained Cutting: Calculating the Stress–Strain State in the Cutting Zone

S. I. Petrushin[a] and A. V. Proskokov[b]

[a] *Tomsk Polytechnic University*

[b] *Yurga Technological Institute, a Branch of Tomsk Polytechnic University*

e-mail: proskokov@tpu.ru

Abstract—A new description of chip formation with a developed plastic-deformation zone is proposed; the tool's geometric parameters are taken into account. A method is proposed for calculating the stress–strain state on the basis of a rigid–plastic model, without hardening of the blank.

DOI: 10.3103/S1068798X10020085

In constrained cutting, the stress–strain state in the chip-formation zone is three-dimensional, especially in cut-layer cross sections for which the cutting depth t and supply S are comparable ($t \approx S$). For forward ($t \gg S$) and inverse ($t \ll S$) chips, plane plastic deformation of two types occurs: 1) a plane stress state; 2) a plane strain state. In the first case, there is no normal stress along the third primary axis, but there is strain; in the second case, there is normal stress, but no strain [1].

Consider the cross section of the chip-formation zone in the direction of chip departure, specified by initial departure angle η (Fig. 1). We may assume that a plane strain state is present if the material in this cross section is constrained by the closest cut layers.

Cross sections close to surfaces that have already been machined and are about to be machined are characterized by a plane stress state. This leads to broadening of the chip (Figs. 1a and 1b). For blocked cutting (channel cutting in turning), the whole chip-formation zone is characterized by a plane strain state (Fig. 1c).

The slip-line field in the plastic chip-formation region for the case where the dynamic front (γ_d) and rear (α) cutter angles in each cross section are zero was considered in [2]. The slip field in the plastic region ($\gamma_d \neq 0$; $\alpha \neq 0$) was considered in [3] (Fig. 2). Formulas for α and β slip lines starting at the front surface were obtained:

for the α lines

$$z_d = \frac{-2l_f\mu_{fo}\ln(l_f - y_d - \mu_{fo}l_f\tan\gamma_d - l_f\tan\gamma_d + y_d\tan\gamma_d - \mu_{fo}l_f)(\tan\gamma_d^2 + 1) - (y_d(\tan\gamma_d)^2 + y_d)}{(-1 + \tan\gamma_d)^2} + C_I;$$

for the β lines (1)

$$z_d = \frac{-2l_f\mu_{fo}\ln(y_d - l_f + \mu_{fo}l_f\tan\gamma_d + y_d\tan\gamma_d - l_f\tan\gamma_d - \mu_{fo}l_f)(\tan\gamma_d^2 + 1) - y_d + y_d(\tan\gamma_d)^2}{(1 + \tan\gamma_d)^2} + C_{II},$$

where μ_{fo} is the frictional coefficient at the tip of the front surface [2].

The boundary α line *OAN* (Fig. 2) passes through the cutter tip and is described by the equation

$$z_d = \frac{-2\mu_{fo}l_f c_\alpha[1 + (\tan\gamma_d)^2] + [1 - (\tan\gamma_d)^2]y_d}{(1 + \tan\gamma_d)^2}, \quad (2)$$

where

$$c_\alpha = \ln\left(\frac{-l_f + y_d + \mu_{fo}l_f\tan\gamma_d + l_f\tan\gamma - y_d\tan\gamma_d + \mu_{fo}l_f}{l_f(-1 + \mu_{fo}\tan\gamma_d + \tan\gamma_d + \mu_{fo})}\right).$$

The boundary β line *EAA*' is perpendicular to the z_d line and leaves point *E*, with the coordinates $y_d = l_{pl}\cos\gamma_d$, $z_d = -l_{pl}\sin\gamma_d$. It is described by the equation

$$z_d = \frac{(2\mu_{fo}c_\beta + y_d) + 4l_{pl}(\cos\gamma_d)^3 - 2y_d(\cos\gamma_d)^2 - 3l_{pl}\cos\gamma_d - l_{pl}\sin\gamma_d}{2\sin\gamma_d\cos\gamma_d + 1}, \quad (3)$$

where

$$c_\beta = \ln\left(\frac{l_{pl}(\cos\gamma_d)^2 - l_f\cos\gamma_d + \mu_{fo}l_f\sin\gamma_d - l_f\sin\gamma_d + l_{pl}\sin\gamma_d\cos\gamma_d - \mu_{fo}l_f\cos\gamma_d}{-l_f\cos\gamma_d + y_d\cos\gamma_d + \mu_{fo}l_f\sin\gamma_d - l_f\sin\gamma_d + y_d\sin\gamma_d - \mu_{fo}l_f\cos\gamma_d}\right).$$

The coordinates of point *A* are obtained by solving Eqs. (2) and (3).

For the boundary α and β lines at the rear cutter surface, when $\alpha \neq 0$, we may write the following formulas [3]:

for the α lines

$$y_d = \frac{(2\mu_{ro}d_\alpha + z_d) + 4h_{pl}(\cos\alpha)^3 - 2z_d(\cos\alpha)^2 - 3h_{pl}\cos\alpha - h_{pl}\sin\alpha}{2\sin\alpha\cos\alpha + 1}; \quad (4)$$

for the β lines

$$y_d = \frac{-2\mu_{ro}h_n d_\beta[1 + (\tan\alpha)^2] + [1 - (\tan\alpha)^2]z_d}{(1 + \tan\alpha)^2}, \quad (5)$$

where

$$d_\alpha = \ln\left(\frac{h_{pl}(\cos\alpha)^2 - h_r\cos\alpha + \mu_{ro}h_r\sin\alpha - h_r\sin\alpha + h_{pl}\sin\alpha\cos\alpha - \mu_{ro}h_r\cos\alpha}{-h_r\cos\alpha + z_d\cos\alpha + \mu_{ro}h_r\sin\alpha - h_r\sin\alpha + z_d\sin\alpha - \mu_{ro}h_r\cos\alpha}\right);$$

$$d_\beta = \ln\left(\frac{-h_r + z_d + \mu_{ro}h_r\tan\alpha + h_r\tan\alpha - z_d\tan\alpha + \mu_{r0}h_r}{h_r(-1 + \mu_{ro}\tan\alpha + \tan\alpha + \mu_{ro})}\right);$$

μ_{ro} is the frictional coefficient at the tip of the rear surface [2].

The position of point *B* is determined by solution of Eqs. (4) and (5). The boundary *CA'K* (Fig. 2) is parallel to line *OAN* at a distance equal to the slip-band thickness; *AA*' = *OC* = *OB*. The method of determining the vertex coordinates for curvilinear plastic triangle *KLM* was presented in [3].

Thus, we may calculate the coordinates of any point on the boundaries of the plastic-deformation zone by means of Eqs. (2)–(5).

In Fig. 3, we plot the boundaries of the plasticity zone for two values of the dynamic front angle. The initial data for the calculation are taken from the experiments in [4]. Decrease in γ_d is accompanied by expansion of the zone of secondary plastic deformation and broadening of the bands in the shear region.

If the front cutter surface is nonplane (with a hardening facet, a chip-coiling groove, etc.), it is very difficult to obtain an analytical solution for the boundary slip lines. We must resort to numerical calculation, with step-by-step construction of an orthogonal slip-line grid in the plastic zone [1].

The stress–strain state in the cutting zone may be calculated by means of Fig. 2. Precise theoretical determination of the stress–strain state is possible for a rigid–plastic model of the blank, without hardening. In that case, the resulting slip-line field in the plastic region is clearly related to the stress state there. Thus, the change in the mean stress $\sigma_{me\,K}$ along the slip lines is proportional to the corresponding angle of rotation [1, 5]

$$\sigma_{me\,K} = \sigma_{me\,L} \pm 2k\omega_{LK}, \quad (6)$$

where *L* and *K* are points of the slip line; ω_{LK} is the angle of slip-line rotation on passing from point *L* to point *K*; *k* is the maximum tangential stress in plastic deformation.

For a plane stress–strain state, $k = 0.5\beta\sigma_y$, where σ_y is the yield point of the blank; the coefficient β depends on the type of stress–strain state: β = 1 for a plane stress state; $\beta = 2/\sqrt{3}$ for a plane strain state.

Knowing the mean stress at the given point of the

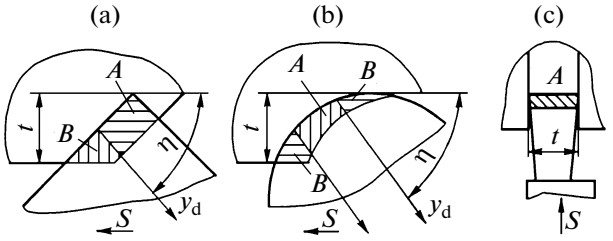

Fig. 1. Regions of plane strain state (*A*) and plane stress state (*B*) in turning: (a) sharp tip; (b) rounded tip; (c) channel.

slip line, we may calculate the stress components for two-dimensional plasticity theory [1]

$$\left.\begin{aligned} \sigma_{y_d} &= \sigma_{me} + k\sin 2\omega; \\ \sigma_{z_d} &= \sigma_{me} - k\sin 2\omega; \\ \tau_{y_d z_d} &= -k\cos 2\omega, \end{aligned}\right\} \qquad (7)$$

where ω is the angle between the tangent to the slip line and the y_d axis at the given point.

We now determine the stress at the left boundary *LKCBD* (Fig. 2). At point *L* on the machined surface, $\sigma_{y_d L} = 0$. (Correspondingly, $\sigma_{z_d L}$ is the compressive primary stress.). From the plasticity condition $\sigma_1 - \sigma_2 = \pm 2k$ for this point, we find that $\sigma_{zL} = -2k$. At this point, the mean stress $\sigma_{me\,L} = (\sigma_1 + \sigma_2)/2 = -k$. The inclination of the tangent to the α slip lines is $\omega_L = \pi/4$.

On passing along the slip line from point *L* to point *K*, according to Eq. (6)

$$\sigma_{me\,K} = -k\left(1 + \frac{\pi}{2} + 2\varphi_K\right).$$

Analogously, for points *C*, *B*, and *D*, the boundary α slip line is

$$\sigma_{me\,C} = \sigma_{me\,K} + 2k\omega_{KC} = -k\left(1 + \frac{\pi}{2} - 2\varphi_K + 2\varphi_C\right);$$

$$\sigma_{me\,B} = \sigma_{me\,C} - k2\omega_{CB} = \sigma_{me\,C} - k2\arcsin(y_d^B/s);$$

$$\sigma_{me\,B} = \sigma_{me\,C} - k2\omega_{CB} = \sigma_{me\,C} - k2\arcsin(y_d^B/s);$$

$$\sigma_{me\,D} = \sigma_{me\,B} + k2\chi_D,$$

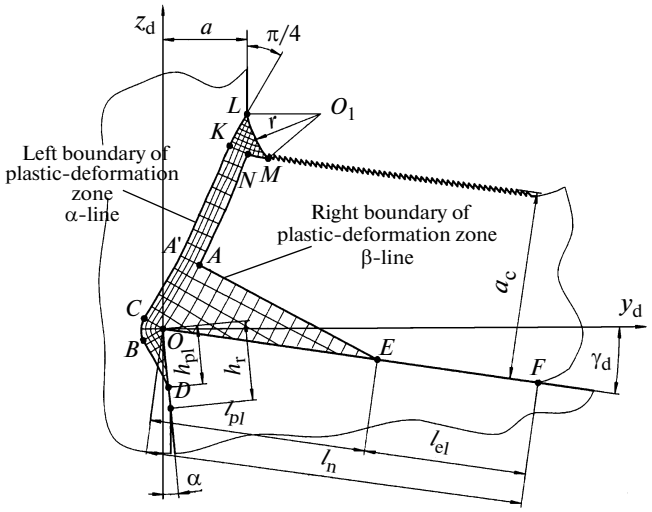

Fig. 2. Slip-line fields when $\gamma_d \neq 0$ and $\alpha \neq 0$.

where χ_D is the inclination of the α slip line at point *D*, which may be determined by taking the derivative of Eq. (4); *s* is the shear-band thickness [2].

Passing along the β line successively from point *K* to points *N* and *M* (Fig. 2), from point *N* along the α line to point *A*, and then along the β line from point *A* to point *E*, we may calculate the mean stress at the points on the right boundary of the plasticity zone.

From Eq. (7), we find the stress components. The stress components at the left and right boundaries of the plastic zone are shown in Figs. 4 and 5 for the corresponding conditions in Fig. 3. Sharp change in the stress–strain state of the blank is observed in the region of the plastic triangle *KLM* and at the cutter tip.

We now calculate the contact stress at the front and read cutter surfaces. This is important in determining the cutting force and the heat released in friction. To this end, we divide the plastic contact section *OE* (Fig. 2) into *n* equal sections of length $y_{dj} = (l_{pl}/n)j$ ($j = 1, 2, ..., n$). The coordinates of the resulting points are substituted into Eq. (1) for the α slip lines, and then the constants of integration C_{1j} are successively determined

$$C_{1j} = y_{dj} - \frac{-2l_f\mu_{fo}\ln(l_f - y_{dj} - \mu_{fo}l_f\tan\gamma_d - l_f\tan\gamma_d + y_{dj}\tan\gamma_d - \mu_{fo}l_f)(\tan\gamma_d^2 + 1) - y_{dj}\tan\gamma_d^2 + y_{dj}}{(-1 + \tan\gamma_d)^2}.$$

Substituting the results into Eq. (1), we obtain *n* equations for the α slip lines leaving the section of the front cutter surface adjacent to plastic contact of the secondary plastic-deformation zone.

By differentiating of each successive α-line equation *j*, with corresponding substitution of the front-surface coordinates, we obtain formulas for the angles of the slip lines at the front surface

$$\varphi_j = \arctan\left(\frac{\mu_{fo}l_f\tan\gamma_d - l_f\tan\gamma_d + y_{dj}\tan\gamma_d - \mu_{fo}l_f - l_f + y_{dj}}{-l_f + y_{dj} + \mu_{fo}l_f\tan\gamma_d + l_f\tan\gamma_d - y_{dj}\tan\gamma_d + \mu_{fo}l_f}\right).$$

The components of the tangential stress are determined from the formula $\tau_{yzj} = -k\cos 2\varphi_j$; the normal stresses are $\sigma_{z_{dj}} = \tau_{y_dz_d}/\mu_j$, where $\mu_j = -\cot\left(\varphi_j + \frac{1}{4}\pi + \gamma_d\right)$.

The second approach to calculating the contact-stress components is their determination from the mean stress on passing along the β line from point *A* to point *E* [6]. To this end, we determine the inclination of the α lines at the boundary *AE* and then the angles of rotation of the α lines on traveling to the front surface. Hence, we determine the corresponding mean stress.

We calculate the contact stresses for the rear cutter surface analogously.

This approach to stress calculation in the chip-formation zone may be verified on the basis of the consistency between the results obtained by the two methods.

In Fig. 6, we show the results for the stress–strain state at the front cutter surface on the basis of the data in Fig. 3. In Fig. 6, σ_z is the normal stress; τ_{yz} is the tangential stress.

The stress–strain state may be calculated by the proposed method on the basis of a special Mathcad program [3]. This program permits the derivation of numerical values for the stress components and graphical representation of the zones.

The algorithm embodied in the program is as follows.

(1) Input the initial data: the yield point σ_y of the blank; the cut-layer thickness *a*; the shrinkage ζ; the front angle γ_d; the rear angle α; and the frictional coefficient μ_{n0} at the cutter tip.

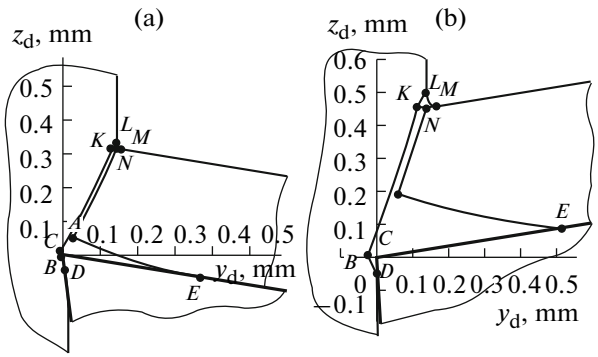

Fig. 3. Boundaries of plasticity zone when $\gamma_d = 10°$ (a) and $-10°$ (b) (30X steel, σ_y = 685 MPa, v = 100 m/min, a = 0.149 mm).

(2) Construct the boundaries of the plasticity zones.

(3) Calculate and plot stress curves along the right and left boundaries of the plasticity zone (σ_{me}, σ_{y_d}, σ_{z_d}, $\tau_{y_dz_d}$).

(4) Calculate and plot the contact-stress distribution at the working surfaces.

In plastic deformation, most materials are hardened. In other words, in the plastic state beyond the yield point, further deformation is associated with increase in the stress required for deformation. This changes the physicomechanical properties of the chip and machined surface (cold working of the surface layer) relative to the remainder of the blank.

On the other hand, plastic deformation, like friction, is a thermoactive process, accompanied by heat formation in the slip-field zone and at the frictional areas. On heating, the blank becomes softer. As yet, we are unable to take account of the resultant influence of these factors on the stress–strain state in the cutting zone, although attempts have been made [5].

We suggest the following approach to constrained cutting, on the basis of the information in [1, 7, 8].

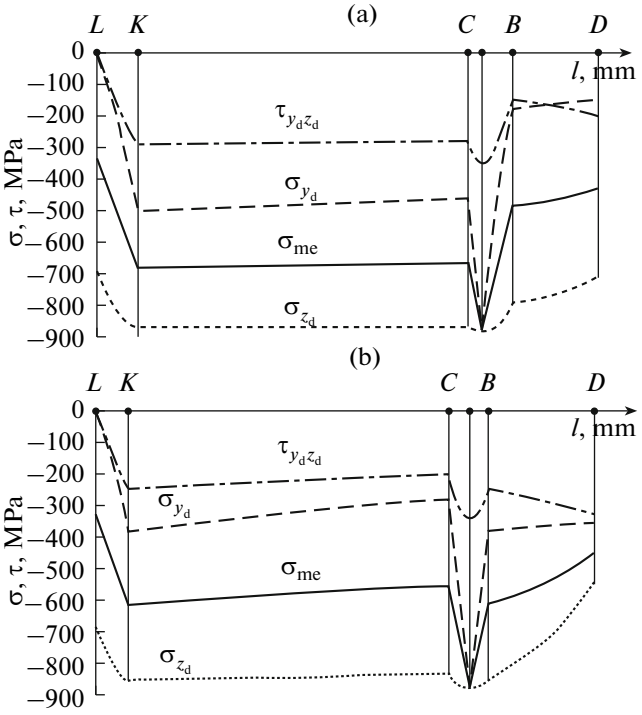

Fig. 4. Stress components along left boundary of plasticity zone.

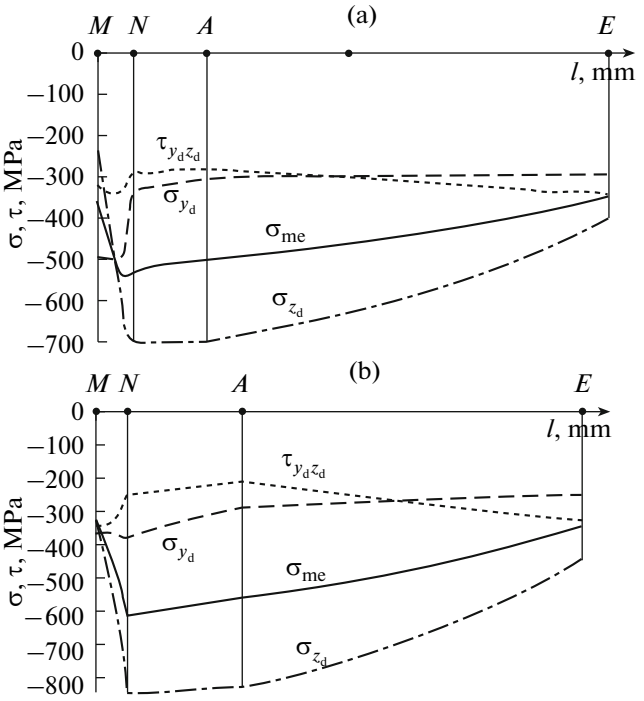

Fig. 5. Stress components along right boundary of plasticity zone.

(1) Description of the geometry of the chip-formation zone, by means of the cutting method, the tool geometry, and the cutting kinematics [7].

(2) Derivation of a chip-formation configuration with a single conditional shear surface and consequent determination of the direction of chip departure and cutting-zone orientation in the dynamic coordinate system [8].

(3) Successive consideration of cross sections of the chip-formation zone at the angle of chip departure and solution of the two-dimensional plasticity-theory problem for each on the basis of the specified characteristics—the type of stress–strain state; the contact-stress distribution; the contact length—so as to determine the contact stress at the front and rear cutter surfaces.

(4) Calculation of the physical components of the cutting force by integration of the contact stress over the contact areas.

(5) Depending on the selected goal, determination of the technological components of the cutting force or solution of thermophysical problems [3], problems of cutter strength and wear [9], and engineering problems.

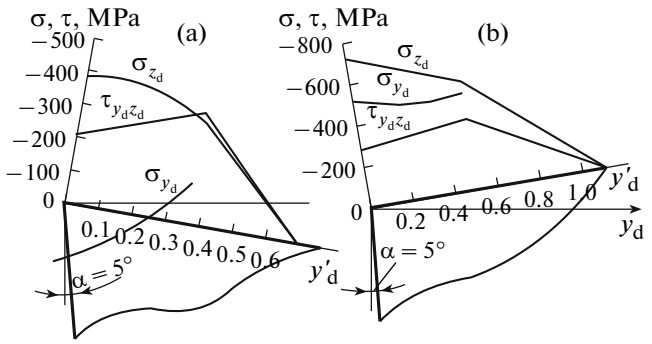

Fig. 6. Contact-stress distribution at front surface.

In subsequent development of the theory, all of the solutions must be formalized as algorithms, on account of the complexity of constrained cutting. A specialized system for automation of the calculations is also required.

REFERENCES

1. Storozhev, M.V. and Popov, E.A., *Teoriya obrabotki metallov davleniem* (Theory of the Pressure Treatment of Metals), Moscow: Mashinostroenie, 1977.
2. Petrushin, S.I. and Proskokov, A.V., Theory of Constrained Cutting: Chip Formation with a Developed Plastic-Deformation Zone, *Vestn. Mashinostr.*, 2010, no. 1.
3. Proskokov, A.V., Improving the Performance of Cutters with Replaceable Hard-Alloy Plates by Regulating the Heat Transfer in the Cutting Zone, *Cand. Sci. Dissertation*, Yurga Technological Institute, Yurga, 2007.
4. Zorev, N.N., *Voprosy mekhaniki protsessa rezaniya metallov* (Mechanics of Metal Cutting), Moscow: Mashgiz, 1956.
5. Petrushin, S.I., *Optimal'noe proektrovanie rabochei chasti rezhushchikh instrumentov* (Optimal Functional Design of Cutting Tools), Tomsk: Izd. TPU, 2008.
6. Gol'dshmidt, M.G., *Deformatsii i napryazheniya pri rezanii metallov* (Strain and Stress in Metal Cutting), Tomsk: STT, 2001.
7. Petrushin, S.I., *Vvedenie v teoriyu nesvobodnogo rezaniya materialov* (Introduction to the Theory of Constrained Cutting), Tomsk: Izd. TPU, 1999.
8. Petrushin, S.I. and Proskokov, A.V., Theory of Constrained Cutting: Geometry of Constrained Cutting, *Vestn. Mashinostr.*, 2009, no. 11, pp. 56–63.
9. Petrushin, S.I. and Proskokov, A.V., Theory of Constrained Cutting: Chip Formation with a Single Conditional Shear Surface, *Vestn. Mashinostr,.*, 2009, no. 12, pp. 58–64.